

## Optical absorption tails and structural disorder in $\text{Sn}_x\text{Ge}_{1-x}\text{Se}_{2.5}$ and other chalcogenide alloy glasses and liquids

A. Ksendzov\* and F. H. Pollak\*

*Department of Physics, Brooklyn College of the City University of New York, Brooklyn, New York 11210*

G. P. Espinosa and J. C. Phillips

*AT&T Bell Laboratories, Murray Hill, New Jersey 07974*

(Received 14 July 1986)

The Urbach slopes  $\sigma$  of optical absorption edges and the glass transition temperatures  $T_g$  in pseudobinary chalcogenide alloy glasses with  $0 \leq x \leq 0.6$  containing predominantly tetrahedral building blocks have been studied as the resistance to shear of the building blocks is varied through the critical composition  $x=0.4$ . The composition dependences of  $\sigma$  and  $T_g$  are nearly parallel, with softening occurring above  $x=0.4$ , in agreement with theoretical expectations. Chemical trends in Urbach slopes of other chalcogenide alloy glasses and liquids are discussed within the framework of constraint theory and a simple statistical model.

### I. INTRODUCTION

Optical absorption tails in crystalline semiconductors and insulators at high temperatures  $T$  exhibit the exponential functional form

$$\alpha = \alpha_0 \exp[(h\nu - E_0)/\sigma], \quad (1)$$

where  $\alpha$  is the absorption coefficient,  $E_0$  is the optical edge energy, and  $\sigma$  describes the logarithmic slope of the absorption tail. The form (1) was discovered phenomenologically by Urbach,<sup>1</sup> and it appears to hold whenever  $\sigma \geq k\Theta_D$ , where  $\Theta_D$  is the Debye temperature.

Because (1) is observed so widely, it would seem that a simple explanation of this behavior should exist. Indeed there have been many theoretical discussions of (1) and attempts have been made to describe disorder-induced band tails using statistical methods.<sup>2,3</sup> Thermal disorder is introduced by techniques used to treat electrical noise in metals, including a Gaussian (random) distribution of disorder. Such approaches are unsatisfactory for two reasons: they do not generally produce the exponential functional form of (1), and they do not generally account quantitatively for observed trends in  $\sigma$ .

Gaussian disorder does not produce the exponential tail (1) exactly. For  $h\nu \ll E_0$  it produces (1) with  $|h\nu - E_0|$  replaced by  $|h\nu - E_0|^\delta$ , with  $\delta = 2 - d/2$ . Thus for dimensionality  $d=3$  one obtains  $\delta = \frac{1}{2}$ , in contrast to the experimental value 1. In a transition region several  $\sigma$  below  $E_0$  a roughly exponential behavior is obtained<sup>2</sup> over about one decade in  $\alpha$ . However, in favorable cases (alkali halides) exponential behavior has been observed<sup>1</sup> over nearly four decades in  $\alpha$ . Many experiments, however, measure  $\alpha$  over only one or two decades and cannot test severely the validity of the fundamental form (1).

A remarkable feature of (1) is that the observed values of  $\sigma = kT^*$  are such that at high  $T$ ,  $T^*$  may be close to  $T$ . This result is not easily explained in the white-noise model

without making special assumptions concerning the valence- and conduction-band-edge electronic deformation potentials, which would seem to be more difficult to justify than (1) itself. In the context of alkali halide Urbach tails Toyozawa and co-workers<sup>2</sup> have attempted to derive the near equality of  $T^*$  and  $T$  in the context of a self-trapped exciton model. While this model is appropriate to alkali and noble-metal halides, it is less appropriate to semiconductors, where exciton radii are larger and exciton-phonon interactions are weaker.

For semiconductors the near equality of  $T^*$  and  $T$  has also been derived<sup>4</sup> assuming that valence- and conduction-band tails are described by acceptor and donor concentrations described by Boltzmann factors. In such derivations it is necessary to assume that the donor and acceptor thermal formation energies are the same as the one-electron energies which determine the optical excitation energy. In general these are not the same, because one should include in the thermal formation energy electronic and structural deformation energies which are different for donor and acceptor states. This problem is particularly serious for amorphous semiconductors where the donor and acceptor states are probably generated by qualitatively different bonding defects in the amorphous network.

From an experimental point of view it is possible to test (1) by comparing  $T^*(x)$  with  $T_g(x)$  in glassy alloys of varying composition  $x$ . Here  $T_g(x)$  is the composition-dependent glass transition temperature of the alloy. In such experiments it is not necessary to test the functional form of (1). Instead the configurational disorder frozen in a  $T = T_g$  is expected to determine  $T^*$ . One can then study both  $T^*$  and  $T_g$  as a function of  $x$  to see whether their near equality is accidental or systematic, and one can attempt to identify the factors responsible for  $T^*(x)$ .

An illuminating discussion of  $T^*(x, T)$  in chalcogenide alloy crystalline and noncrystalline semiconductors has

been given by Ihm.<sup>5</sup> He points out the close relation between  $T^*(x, T)$  and the underlying molecular structure even in amorphous or glassy semiconductors such as  $g\text{-As}_x\text{Se}_{1-x}$  and  $g\text{-Ge}_x\text{Se}_{1-x}$  alloys. He notes that the general relationship between  $T^*$  and  $T_g$  is complex in these alloys, although most of the qualitative features are explained by assuming that the layered-compound crystal structure persists locally in the alloys near the crystalline compositions ( $\text{As}_2\text{Se}_3$  and  $\text{GeSe}_2$ ).

Experimental data<sup>6,7</sup> for  $T^*(x, 293 \text{ K})/T_g(x)$  for these binary alloys are summarized in Fig. 1. Note the nearly equal minima in  $T^*/T_g$  at the crystalline compositions where  $T^*/T_g = 1.22 \pm 0.05$ . The origin of these minima may be chemical ordering of the  $A_xB_{1-x}$  alloy to form branched rings  $A_nB_n$ . Another possible explanation is that two kinds of building blocks must exist in these alloys at compositions other than the crystalline composition. In  $\text{As}_x\text{Se}_{1-x}$  alloys there could be  $\text{Se}_n$  chains or  $\text{As}(\text{Se}_{1/2})_3$  pyramids, while in  $\text{Ge}_x\text{Se}_{1-x}$  alloys one could have  $\text{Se}_n$  chains or  $\text{Ge}(\text{Se}_{1/2})_4$  tetrahedra.

Ihm has suggested<sup>5</sup> that it would be interesting to study  $T^*(x)/T_g(x)$  in a system where  $T_g(x)$  varies but the fractions of building blocks stay fixed, rather than vary, as in  $\text{As}_x\text{Se}_{1-x}$  (all chains at  $x=0$ , all pyramids at  $x=0.4$ ) or  $\text{Ge}_x\text{Se}_{1-x}$ . The fractions of building blocks can be kept fixed in a pseudobinary alloy such as  $\text{Sn}_x\text{Ge}_{1-x}\text{Se}_{2.5}$  which we study here. In this way we expect to obtain more information on the structural origin of the defects responsible for the Urbach tails. Note that in these alloys it has been shown<sup>8,9</sup> that for  $0 \leq x \leq 0.6$  water quenching produces samples with both Sn and Ge at tetrahedral sites. Also note that the composition of these alloys is slightly Se rich (relative to  $\text{GeSe}_2$ ) in order to avoid crystallization of any significant fraction of the sample, which might lead to phase separation and an unknown composition of the glassy residue.

## II. EXPERIMENTAL PROCEDURES

### A. Sample preparation

Appropriate amounts of high-purity Ge, Sn, and Se (99.999% purity) were combined to yield a total sample

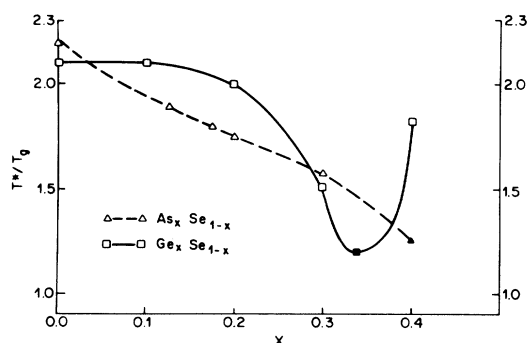


FIG. 1. Chemical trends in  $\sigma/kT_g = T^*/T_g$  in binary chalcogenide alloys; data from Refs. 6 and 7. The stoichiometric alloy compositions are indicated by solid symbols.

weighing 0.50 g. The selenium was first vacuum melted to remove possible volatile contaminants. The weighed material was carefully transferred into a rectangular fused silica tube with a  $4 \times 2 \text{ mm}^2$  inner cross section which was then sealed off to a length of 4 cm under vacuum. The samples were heated from room temperature to  $900^\circ\text{C}$  and held there for about 24 h during which time the ampoules were occasionally shaken and inverted to homogenize. This treatment was followed by a room-temperature water quench. The resulting rectangular pieces of glass were convenient to cut and polish.

For optical measurements one half of each sample was ground and polished on both sides so that the final thickness was 0.2–0.4 mm. The grinding was performed on the glass plate using 600-grit boron carbide powder. The polishing was done using first  $1\text{-}\mu\text{m}$  and then  $0.05\text{-}\mu\text{m}$  alumina powder on rotating Politex pads. Typically a  $30\text{-}\mu\text{m}$  layer was removed by polishing with  $1\text{-}\mu\text{m}$  powder and  $10 \mu\text{m}$  by polishing with  $0.05\text{-}\mu\text{m}$  powder.

To make sure that the polishing procedure does not affect the optical properties of our samples measurements were made on two parts of the same sample: one “as-grown”—a plane splinter of glass approximately 0.7 mm thick, and another part that was polished. The two yielded spectra identical within experimental error.

### B. Wavelength-modulated absorption

The wavelength-modulation technique<sup>10</sup> has previously been used<sup>7</sup> to study Urbach tails in  $\text{Ge}_x\text{Se}_{1-x}$  glasses in transmission. Here we use the technique to measure the absorption coefficient  $\alpha$ . From (1) we have ( $E = h\nu$ )

$$d\alpha/dE = \alpha/\sigma \quad (2)$$

and we can show that

$$d\alpha/dE = \lambda^2[(d \ln I_T/d\lambda)_{\text{SO}} - (d \ln I_T/d\lambda)_{\text{SI}}]/het, \quad (3)$$

where  $I_T$  is the intensity of light of wavelength  $\lambda$  transmitted by the sample of thickness  $t$ , and the measurements are made with the single-beam method<sup>7,10</sup> with the sample out of (SO) or in (SI) the beam. The quantity  $\sigma$  is determined from the slope of a logarithmic plot of  $d\alpha/dE$  against  $E$ , because this slope is the same as that of  $\alpha$ .

For each sample studied optically, differential thermal analysis (DTA) was performed using a duPont 990 analyzer; representative curves are shown in Fig. 2. The samples analyzed weighed about 40 mg and were contained in a fused-silica cup under an argon atmosphere. The glass transitions ( $T_g$ ) are apparent at about  $275^\circ\text{C}$  with the crystallization exotherm ( $T_c$ ) appearing at about  $450^\circ\text{C}$  and  $400^\circ\text{C}$ . The weak endotherm of the  $x=0.3$  curve at  $520^\circ\text{C}$  probably results from the melting of some minor constituent of the multiphase crystalline material formed upon the crystallization of the homogeneous glass.

In Fig. 3 we plot  $d\alpha/dE$  as a function of photon energy  $E$  for the  $g\text{-Sn}_x\text{Ge}_{1-x}\text{Se}_{2.5}$  samples that we studied. In each case  $\alpha$  is linear on a semilogarithmic scale over at least a decade in  $\alpha$ , as expected for an Urbach tail. Over this region a least-squares fit to a linear relationship has

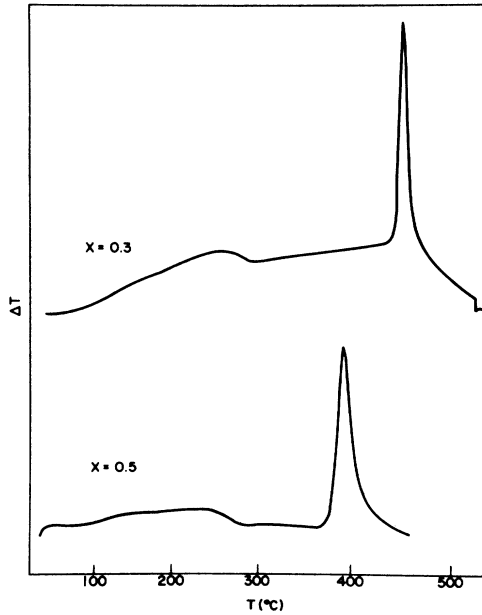


FIG. 2. Differential thermal analysis traces for  $\text{Sn}_x\text{Ge}_{1-x}\text{Se}_{2.5}$  glasses, for  $x=0.3$  and  $x=0.5$ . Initial, central, and final glass transition temperatures were estimated from these traces graphically by constructing tangents to the rising and falling slopes of the broad glass transition peak. For  $x=0.5$  the initial (final) temperatures correspond to the breaks in slope near  $255^\circ\text{C}$  and  $290^\circ\text{C}$ , respectively.

been made. The obtained values of  $\sigma(x)$  are compared with those of  $T_g(x)$  in Fig. 4. Also shown in Fig. 4 is  $T^*(x)/T_g(x)$ , where the midpoints of the transition are used to define  $T_g$ .

We note that in Fig. 3 the relative positions of the edges are not a monotonic function of composition. This may seem surprising, but similar oscillations are observed in relative strengths of Raman bands and Mössbauer site populations.<sup>8</sup> These oscillations have been explained in terms of site distributions of Sn atoms compared to Ge atoms. Similar mechanisms may explain the oscillations in relative edge positions in Fig. 3.

### III. DISCUSSION

Over the composition range  $x$  studied both  $T^*$  and  $T_g$  decrease with increasing  $x$ , with  $T^*$  decreasing by about 15% while  $T_g$  (measured in K) decreases by about 5%. Thus the behavior is qualitatively similar in both cases, in contradistinction to  $\text{As}_x\text{Se}_{1-x}$  alloys,<sup>6</sup> where  $T^*$  decreases and  $T_g$  increases with  $x$  increasing in the interval  $0 \leq x \leq 0.4$ . The qualitative similarity probably is due to a constant fraction of tetrahedral building blocks, as suggested by Ihm.<sup>5</sup>

Returning to Fig. 1, we note that both stoichiometric binary glasses exhibit values of  $T^*/T_g$  close to the value of 1.3 recently calculated in the context of a quantum well model.<sup>11</sup> In  $g\text{-Se}$ , on the other hand,  $T^*/T$  is approximately equal to 2.1. This high ratio is found in liquid Se

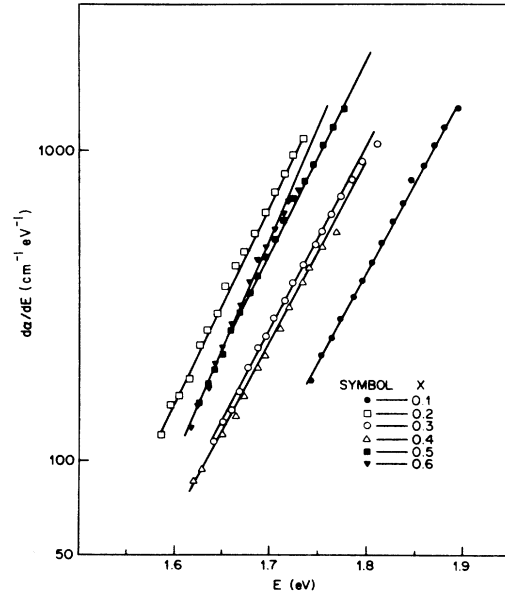


FIG. 3. Experimental results for Urbach slopes in  $\text{Sn}_x\text{Ge}_{1-x}\text{Se}_{2.5}$  glasses.

over a wide temperature range ( $500 \leq T \leq 900$  K) as well.<sup>12</sup>

In view of the structural correlations for layered stoichiometric glasses discussed by Ihm<sup>5</sup> as well as those found here, we suggest a structural model for  $g\text{-Se}$ . The defects responsible for the Urbach tail cannot be only bro-

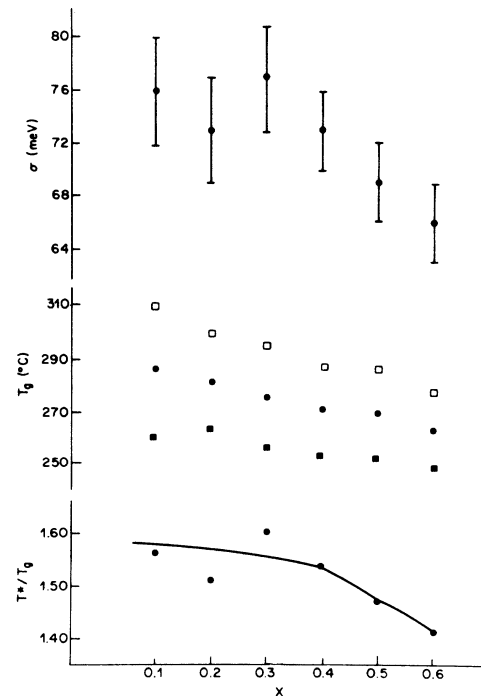


FIG. 4. Summary of chemical trends in  $\sigma$ ,  $T_g$ , and  $T^*/T_g$  as a function of  $x$  in  $\text{Sn}_x\text{Ge}_{1-x}\text{Se}_{2.5}$  glasses.

ken bonds, because studies of the Urbach edge in liquid S and Se have shown<sup>12</sup> that isolated broken bonds occur only at very high temperatures ( $\geq 700$  K). We suppose, as others have done<sup>12</sup> that *g*-Se consists of a mixture of chains and rings. The chains may form cylindrical bundles and the rings may be stacked as in the various crystalline forms of Se. Both groups or clusters are "floppy" (only two constraints per atom) so far as nearest- and next-nearest-neighbor (bond stretching and bending) forces are concerned.<sup>10,13</sup> Within either kind of cluster we assume that structural defects (concentration  $N_d$ ) (such as chain kinks) occur which produce valence- or conduction-band-edge "defect" states. However, because of the floppy or underconstrained nature of the chains, most of these kinks form pairs on adjacent chains. The electronic states associated with paired defects are assumed to lie too close to the band edge to contribute significantly to the optical tail. The latter is determined by the residual unpaired defect states, whose population is supposed to be proportional to  $N_d^{1/2}$ . With  $N_d \propto \exp[(h\nu - E_0)/nkT_g]$  this gives  $N_d^{1/2} \propto \exp[(h\nu - E_0)/2nkT_g]$ . Thus, when the system is sufficiently underconstrained,  $T^* = 2nT_g$ , whereas at the stoichiometric compositions  $T^* = nT_g$ , with the ideality factor  $n = 1.3$  according to the quantum-well model.<sup>11</sup> The value  $T^*/T_g = 2.1$  in glassy and liquid Se is not quite  $2n$ , indicating that the fluctuations are nearly (but not perfectly) free or random.

The increase in the ideality factor  $n$  from 1.2 in *g*-As<sub>2</sub>Se<sub>3</sub> and *g*-GeSe<sub>2</sub> to  $n = 2.1$  in glassy and liquid S and Se is primarily a kinetic effect associated with defect pairing in our model. This kinetic effect can be interpreted also as an effective reduction (due to pairing) in the energy  $\Delta E = h\nu - E_0$  available to determine the active-defect concentration. The most striking aspect of this kinetic ef-

fect is the wide temperature range it spans. For liquid Se an activated increase in  $\sigma$  is observed<sup>12</sup> above 700 K, corresponding to further increases in  $n$ . These may occur because of further isolated defect formation due to defect-pair unpinning, possibly by bond breaking.<sup>12</sup>

The ratio of  $T^*/T_g$  is nearly constant for Sn<sub>*x*</sub>Ge<sub>1-*x*</sub>Se<sub>2.5</sub> alloys in the range  $0 \leq x \leq 0.4$ . In this region the network is dominated by rigid or overconstrained clusters.<sup>8,10,13</sup> For  $x > 0.4$ ,  $T^*(x)$  decreases more rapidly than  $T_g(x)$ . This more rapid decrease may reflect an increasing ability of the glass to relax and optimize bent Se—Se—Se bonds because the large chemically ordered clusters (such as layerlike crystalline fragments) have become "floppy."<sup>13</sup> (Note here that the actual *relative* error bars in Fig. 4 are much smaller than the error bars for any single measurement.)

In conclusion, considerable information is contained in chemical trends in Urbach slopes in binary and pseudo-binary chalcogenide alloy glasses. These trends indicate the extent to which local bond reconstruction depends on overall network rigidity<sup>10,13</sup> as well as the structure of the local molecular units themselves.<sup>5</sup> Our discussion of chemical trends in the kinetic ideality factor  $n = T^*/T$  explains the experimental range in glasses and liquids from  $n = 1.2$  in *g*-As<sub>2</sub>Se<sub>3</sub> and *g*-GeSe<sub>2</sub> to  $n = 2.1$  in glassy and liquid S and Se. This large change is probably the result of topologically distinct defects in the elemental and compound composition glasses. The elemental defect is an isolated chain kink,<sup>12</sup> while the defect in stoichiometric glasses is a homopolar (broken chemical order) bond.<sup>5</sup> We believe that the present kinetic and topological treatment is both more conclusive and more illuminating than previous theoretical discussions based on white noise.<sup>2,3</sup>

\*Also at Physics Department, Graduate School and University Center, City University of New York, NY 10036.

<sup>1</sup>F. Urbach, *Phys. Rev.* **92**, 1324 (1953).

<sup>2</sup>Y. Toyozawa, *Prog. Theor. Phys.* **20**, 53 (1958); **22**, 455 (1959); H. Sumi and Y. Toyozawa, *J. Phys. Soc. Jpn.* **31**, 342 (1971); S. Abe and Y. Toyozawa, *ibid.* **50**, 2185 (1981); M. Schreiber and Y. Toyozawa, *ibid.* **51**, 1528 (1982); **51**, 1537 (1982); **51**, 1544 (1982).

<sup>3</sup>B. I. Halperin and M. Lax, *Phys. Rev.* **148**, 722 (1966).

<sup>4</sup>I. Z. Kostadinov, *J. Phys. C* **10**, L263 (1977).

<sup>5</sup>J. Ihm and J. C. Phillips, *Phys. Rev. B* **27**, 7803 (1983); J. Ihm, *Solid State Commun.* **53**, 293 (1985); *J. Phys. C* **18**, 4741 (1985).

<sup>6</sup>R. S. Sussmann, I. G. Austin, and T. M. Searle, *J. Phys. C* **8**, L182 (1975); M. B. Myers and E. J. Felty, *Mater. Res. Bull.* **2**, 535 (1967).

<sup>7</sup>H. Oheda, *Jpn. J. Appl. Phys.* **10**, 1973 (1979); R. Azoulay, H. Thibierge, and A. Brenac, *J. Non-Cryst. Solids* **18**, 33 (1975).

<sup>8</sup>M. Stevens, J. Grothaus, and P. Boolchand, *Solid State Commun.* **47**, 199 (1983).

<sup>9</sup>K. Murase and T. Fukunaga, *Optical Effects in Amorphous Semiconductors*, Proceedings of the International Topical Conference on Optical Effects in Amorphous Semiconductors, AIP Conf. Proc. No. 120, edited by P. C. Taylor and S.

G. Bishop (AIP, New York, 1984), p. 449.

<sup>10</sup>J. C. Phillips, *Solid State Commun.* **47**, 203 (1983).

<sup>11</sup>C. T. Chan, S. G. Louie, and J. C. Phillips, following paper, *Phys. Rev. B* **35**, 2744 (1987).

<sup>12</sup>J. Rabit and J. C. Perron, *Phys. Status Solidi B* **65**, 255 (1974).

At very high temperatures (above 700 K)  $T^*$  increases superlinearly in liquid Se, suggesting structural breakdown either of clusters or of bonds. In liquid S at very high temperatures (also above 700 K) direct optical evidence for bond breaking has been reported by G. Weser, F. Hensel, and W. W. Warren, *Ber. Bunsen Gesell. Phys. Chemie* **82**, 588 (1978). Their data also show at 140°C an absorption edge exponential over five decades. Finally, we note that a plausible structural model for chain kinks in S and Se is the local defect complex of onefold and threefold coordinated atoms described by S. Itoh and K. Nakao, *J. Phys. Soc. Jpn.* **55**, 268 (1986). Because of the large kink angle ( $\sim 120^\circ$ ), these units could act as crosslinks connecting otherwise largely distinct clusters. For other experimental data bearing on chain ends (onefold coordinated atoms) and kinks, see M. Edeling, R. W. Schmutzler, and F. Hensel, *Philos. Mag. B* **39**, 547 (1979) and W. W. Warren, Jr., and R. Dupree, *Phys. Rev. B* **22**, 2257 (1980).

<sup>13</sup>J. C. Phillips and M. F. Thorpe, *Solid State Commun.* **53**, 699 (1985).